NANO LETTERS

pubs.acs.org/NanoLett

Letter

Zero Field Splitting of Heavy-Hole States in Quantum Dots

Georgios Katsaros,* Josip Kukučka, Lada Vukušić, Hannes Watzinger, Fei Gao, Ting Wang, Jian-Jun Zhang, and Karsten Held

Cite This: *Nano Lett.* 2020, 20, 5201−5206

Read Online

ACCESS | Metrics & More | Article Recommendations

ABSTRACT: Using inelastic cotunneling spectroscopy we observe a zero field splitting within the spin triplet manifold of Ge hut wire quantum dots. The states with spin ±1 in the confinement direction are energetically favored by up to 55 μeV compared to the spin 0 triplet state because of the strong spin−orbit coupling. The reported effect should be observable in a broad class of strongly confined hole quantum-dot systems and might need to be considered when operating hole spin qubits.

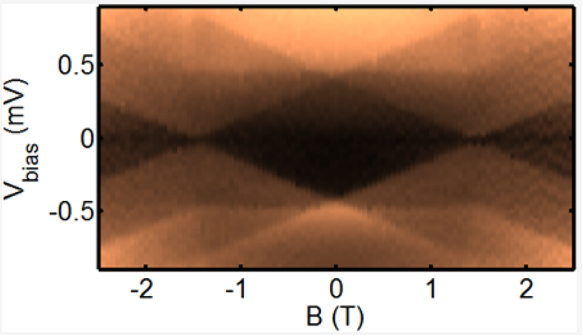

KEYWORDS: *quantum dots, holes, spin−orbit, zero field splitting*

Hole states in semiconductor quantum dots have gained increasing interest in the past few years as promising candidates for spin qubits due to their strong spin orbit coupling (SOC).[1−4] Thanks to the SOC one now has a full-fledged electrical control of the hole spins,[5−8] either via the electric-dipole spin resonance,[9] *g*-tensor modulation,[10] or both.[11] Further, Rabi frequencies exceed 100 MHz[6,7] and reflectometry measurements reveal spin relaxation times of 0,1 −1 ms,[12,13] which underlies the big potential of hole spins as viable qubits.

Despite the fact that a hole is simply a missing electron, their spins behave strikingly different than their electron counterparts.[14] While the electron spin does not correlate with the direction of motion in typical semiconductors given their weak SOC [Figure 1(a)], the hole pseudospin points in the same direction as the momentum [Figure 1(b)] already for bulk materials. This can be described by the Luttinger−Kohn Hamiltonian[15,16] for holes near the Γ point of the valence band, imposing a coupling between the momentum and the hole pseudospin.

By introducing a strong confinement potential creating a quantum well, the heavy-hole (HH) light-hole (LH) degeneracy is lifted and the pseudospin changes its direction. For the HH states, which become energetically favorable, the pseudospin now points perpendicular to the momentum, i.e., in the direction of strong confinement [Figure 1(c)].[14] This implies that HHs confined in quasi two-dimensional quantum dots (QDs), i.e., artificial atoms with strong confinement in one dimension, show spin anisotropy and could thus manifest similar effects as atoms show in the presence of a magneto-crystalline anisotropy, i.e., a magnetic anisotropy leading to a zero field splitting (ZFS). However, to the best of our knowledge hitherto, no ZFS has been observed for quantum dots.

For adatoms, on the other hand, ZFS studies have been at the focus of intense research as the magnetic anisotropy provides directionality and stability to the spin, which is the key for realizing nanoscale magnets. Scanning tunneling microscopy measurements have been used to reveal the magnetic anisotropy for several adatoms on surfaces and to understand how the local environment can influence it.[17−21] ZFS as high as 58 meV, originating from the atomic spin−orbit interaction, have been reported.[17]

Here, we use inelastic cotunneling (CT) to extract information about confined HH states. Figure 2(d) visualizes the inelastic CT, a higher order process in the tunneling rate where both an electron is removed from the QD and added to it in the same CT process. It is inelastic if the energy of the QD changes, which is possible if the applied voltage (red double arrow in Figure 2(d)) matches the level or Zeeman splitting in the QD (green double arrow). A hole−hole interaction strength of 275 μeV, similar to that of GaAs,[22] is reported. We have furthermore investigated the spin anisotropy of HH states confined in quasi two-dimensional QDs. We measure a

Received: April 3, 2020
Revised: May 30, 2020
Published: June 1, 2020

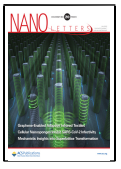

https://dx.doi.org/10.1021/acs.nanolett.0c01466
Nano Lett. 2020, 20, 5201−5206

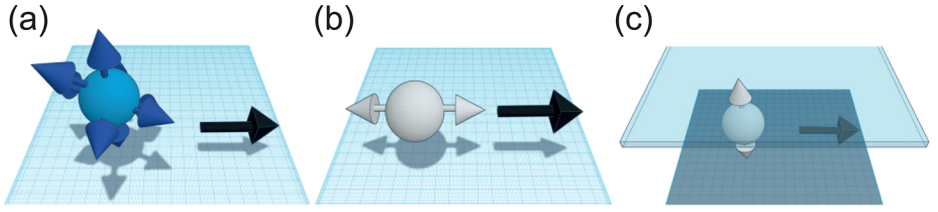

Figure 1. (color online) Spin physics for (a) electrons, (b) bulk holes, and (c) confined HH states. While for electrons the momentum (black arrows) and the spin are not correlated, for bulk holes the pseudospin is locked in the direction of motion because of their strong valence band SOC. By confining holes in two dimensions, HHs become energetically favorable and their pseudospin points in the confinement direction, perpendicular to their momentum.

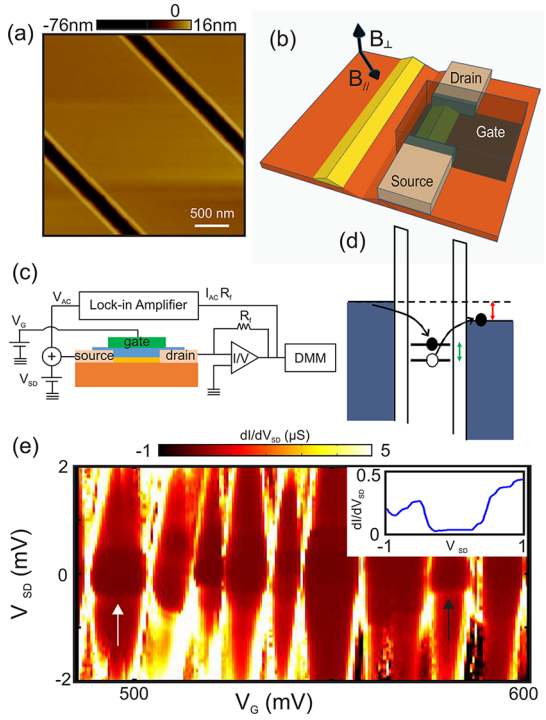

Figure 2. (color online) (a) Atomic force microscopy image showing parallel Ge HWs grown at the edges of trenches etched in the silicon wafers prior to growth. (b) Schematic showing the device geometry and the direction of the applied magnetic field. The HW is covered with a thin layer of hafnia (not shown), before the top gate is deposited. (c) Schematic illustration of the measurement setup. (d) Schematics showing the onset condition for inelastic cotunnelling when the applied bias (red double arrow) is equal to either the orbital level separation or the Zeeman splitting (green double arrow). (e) Differential conductance dI/dV_{SD} as a function of gate voltage V_G and source-drain voltage V_{SD} at $B = 0$ T. The arrows indicate the position of two inelastic CT steps. The inset shows the dI/dV_{SD} as a function of source-drain voltage V_{SD} at the position of the white arrow.

ZFS of up to 55 μeV for the excited triplet states confined in a QD with an even hole occupation. The evolution of the triplet states both for perpendicular and parallel magnetic fields is in very good agreement with the anisotropic Hamiltonian for the spin-triplet.

The QDs used for this study are fabricated in Ge hut wires (HWs) grown by molecular beam epitaxy.[23,24] These HWs are site-controlled as they are grown on Si wafers with predifined trenches [Figure 2(a, b)]. The detailed description of the growth conditions can be found in ref 23. They have a height of about 3.8 nm and a width of approximately 38 nm. Due to the strong confinement and compressive strain, the degeneracy between the HH and LH is lifted, leading to confined HH states.[25,26] The measured devices have been fabricated by electron beam lithography, metal, and atomic layer deposition. Pt has been chosen as a source and drain material due to its high work function; 25 nm of Pt is deposited on the hut wires after a 10 s BHF etching step in order to remove the native silicon oxide. The spacing between the two Pt leads is about 50 nm. The gate electrode consists of 3 nm Ti plus 25 nm Pt; 80 cycles of hafnium oxide deposited at 150 °C by means of atomic layer deposition serve as the gate oxide. The measurements have been performed in a ^{3}He/^{4}He refrigerator with an effective electron temperature of 100 mK. The electronic setup is displayed in Figure 2(e). Let us also note that the DC lines are filtered with pi filters at room temperature, LC filters at the mixing chamber stage and RC filters on the printed circuit board on which the sample is mounted. Two nominally identical devices from the fabricational point of view have been investigated in this study.

At low temperatures, transport through QDs is dominated by Coulomb blockade (CB), which leads to single electron transport. The stability diagram of a QD device with the characteristic Coulomb diamonds can be seen in Figure 2(e). However, due to second-order elastic CT processes the conductance within the Coulomb diamonds does not drop to zero.[27,28] At zero magnetic field, once the energy due to the bias voltage across the QD exceeds the orbital level separation, $|eV_{SD}| > E_{ORB}$, the inelastic CT process leaves the QD in the excited orbital state ($e > 0$ denotes the elementary charge). The onset of inelastic CT is observed as a step in the differential conductance, dI/dV_{SD}, at $eV_{SD} = \pm E_{ORB}$,[27−29] indicated by black and white arrows in Figure 2(e).

Inelastic CT is an excellent tool for magnetotransport spectroscopy measurements as the step width is not lifetime limited but depends only on the effective temperature.[28] We first use it to extract information related to the strength of hole−hole interactions within a QD. When a QD confines an odd number of holes, the ground state is a (doubly degenerate) spin-doublet. On the other hand, with an even number of holes the ground state of the QD is a singlet state (assuming that the exchange coupling is weaker than the level splitting). Here, the two holes occupy the same (lowest in energy) orbital state with their pseudospins being antiparallel. The first excited states are the triplet states for which one hole occupies a higher orbital. This not only costs a higher energy for the orbital occupation but also gains some Coulomb repulsion energy compared to the singlet state.[22,31] By comparing the difference between the singlet−triplet energy E_{ST} and the orbital level separation E_{ORB}, one can thus obtain useful information about the strength of hole−hole interactions.

https://dx.doi.org/10.1021/acs.nanolett.0c01466
Nano Lett. 2020, 20, 5201−5206

In order to conclude about the even/odd occupancy of the QD we investigate the evolution of the CT steps. For an odd number of holes, a magnetic field B lifts the spin degeneracy of the doublet state by the Zeeman energy $E_Z = g\mu_B B$, where g and μ_B are the hole g-factor and Bohr magneton, respectively. Once the energy due to the bias voltage across the QD exceeds the Zeeman energy, $|eV_{SD}| > E_Z$, the inelastic CT processes can flip the QD spin, leaving the QD in the excited spin state. This is visible as a step in Figure 3(a). For the zero magnetic field

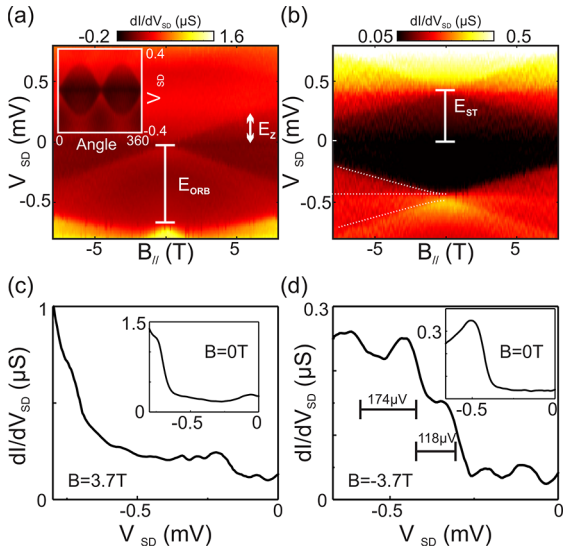

Figure 3. (color online) (a) dI/dV_{SD} as a function of $B_{\|}$ and V_{SD} at V_G = 510.5 mV for which the QD is in a spin-doublet ground state. Inset: dI/dV_{SD} at B = 1 T as a function of V_{SD} and magnetic field angle, from which a strong g-factor anisotropy of about 7.5 ($g_{\|}$ = 0.56 ± 0.06 and $g_{\perp}$ = 4.17 ± 0.22) can be extracted similar to that in ref 26. This anisotropy is due to the HH character of the confined states.[25,26,30] (b) dI/dV_{SD} as a function of $B_{\|}$ and V_{SD} at V_G = 528.3 mV for which the QD now has a singlet ground state with $g_{\|}$ = 0.57 ± 0.01 and $g_{\perp}$ = 4.56 ± 0.16. The dotted lines are the calculations from Figure 4(b) (below) for $B_{\perp} \leq 0$, but reverted because the CT is at a negative V_{SD} bias. (c, d) Line traces illustrating the CT steps at B = 3.7 T and B = −3.7 T, for the odd and even QD occupancy, respectively. The insets illustrate the B = 0 T traces from which E_{ORB} = 690 μeV and E_{ST} = 415 μeV are extracted. The unequal spacing between the triplet states in (d) of 174−118 μeV reveals a ZFS of 55 μeV when rounded within our error of 5 μeV.

the observed feature corresponds to the first orbital excited state from which an orbital level separation E_{ORB} of 690 μeV can be extracted. For an even number of holes, on the other hand, the magnetic field should split the three triplet states, and three inelastic cotunneling steps should be observed (note that the other state involved, the ground state singlet, does not split in a magnetic field). Indeed this behavior can be observed in Figures 3(b) and (d). In this case the feature at zero field corresponds to the energy of the triplet states. The measured singlet triplet energy separation E_{ST} is 415 μeV. The difference $E_{ORB} - E_{ST}$ = 275 μeV corresponds to the Coulomb interaction energy and is similar to what has been reported for GaAs QDs.[22]

By inspecting carefully the behavior of the triplet states in Figure 3(b), it can be seen that the triplets are not equally spaced (Figure 3(d)); it actually seems that the three triplet states (marked by three dashed lines) are not degenerate at B = 0 T. Ge is known to have a very strong atomistic (valence band) SOC which leads to the HH spin pointing in the perpendicular direction of Figure 1 (c). We can envisage the triplet state as being made up of two such HH spins. This or, even more general, any triplet with an anisotropy in the ⊥-direction of Figure 2(b) can be described by the following Hamiltonian for the triplet spin $\mathbf{S}$ (see, e.g., refs 32 and 33):

$$H = -J/2\mathbf{SS} + g_{\perp}\mu_B S_{\perp} B_{\perp} + g_{\|}\mu_B S_{\|} B_{\|} - DS_{\perp}^2 \quad (1)$$

Here, $S_{\perp}$ and $S_{\|}$ are the projections in the ⊥- and ||-direction of Figure 2(b), and the terms of the Hamiltonian are from right to left are as follows. The magnetic anisotropy term is $DS_{\perp}^2$ which makes it preferably by an energy D to align the triplet spin-1 in the ⊥-direction with strongest confinement. Its origin will be discussed in the next paragraph. The next two terms describe the Zeeman term with the magnetic field in the two directions, $B_{\perp}$ and $B_{\|}$, coupling through different (anisotropic) $g_{\perp}$ and $g_{\|}$-factors. Finally, we also include the exchange term J which differentiates singlet and triplet but is not relevant in the following as we concentrate on the magnetic field dependence of the triplet states ($\mathbf{S}$ = 1 fixed) only.

From the effective Hamiltonian (1) for the triplet states we cannot distinguish the origin of the magnetic anisotropy. It might be due to (i) shape anisotropy caused by dipole interactions,[33] (ii) single ion (single quantum dot) anisotropy caused by SOC-induced transitions to excited (virtual) states,[32,33] or (iii) a SOC-induced anisotropic exchange J_A.[34,35]

The last microscopic origin (iii) is certainly the most natural if we think of the triplet spin-1 state as being made up out of two HH spin ±3/2 states, which we can describe as two coupled pseudospin-1/2, $\mathbf{S}_1$ and $\mathbf{S}_2$. Given that these pseudospins actually describe HH spin ±3/2 states (or the strong SOC coupling from a general perspective), the coupling of these pseudospins has to be anisotropic, i.e., $H = -J\mathbf{S}_1\mathbf{S}_2 - J_A S_{1\perp} S_{2\perp}$. This reduces to eq 1 with $\mathbf{S} = \mathbf{S}_1 + \mathbf{S}_2$ and $D = J_A/2$ in the triplet subspace, up to a constant. While (i) is unlikely as the dipole−dipole interaction is weak so that many spins have to be involved, we cannot distinguish between (ii) and (iii). These are different mechanisms, resulting both in the same Hamiltonian (1) and explaining both the ZFS.

The eigenstates of Hamiltonian (1) can be easily calculated and are shown in Figure 4 for a magnetic field applied once in the ⊥- and once in the ||-direction. For B = 0 the two states with $S_{\perp} = \pm 1$ have a by $-D$ smaller energy than the third triplet state with $S_{\perp}$ = 0. Hence, the lowest triplet state is doubly degenerate and the remaining one singly degenerate in Figure 4. Applying now a magnetic field in the anisotropy direction, $B_{\perp}$ Zeeman splits the doublet and leaves the singly degenerate $S_{\perp}$ = 0 state untouched (Figure 4 (a)), with $E_{S+} - E_{S-} = 2g_{\perp}\mu_B B$.

The situation with the magnetic field $B_{\|}$ orthogonal to the anisotropy direction is somewhat more complicated. Here, for small $B_{\|}$, the eigenstates are still predominately $S_{\perp} = \pm 1, 0$ with only a small, perturbative readmixture $\sim g_{\|}\mu B_{\|}/D$ as the magnetic field tries to align the spins in the ||-direction. This linear readmixture of the eigenstates leads to a quadratic change of the energy eigenvalues in Figure 4 (b) for $g_{\|}\mu B_{\|} \ll D$. For large $g_{\|}\mu B_{\|} \gg D$, the usual Zeeman splitting of the triplet states into $S_{\|} = \pm 1, 0$ is recovered as the HH pseudo spins now reorient along $B_{\|}$. This is in very good agreement with the data shown in Figure 3(b), even though we have not adjusted the parameters but extracted these experimentally

https://dx.doi.org/10.1021/acs.nanolett.0c01466
Nano Lett. 2020, 20, 5201−5206

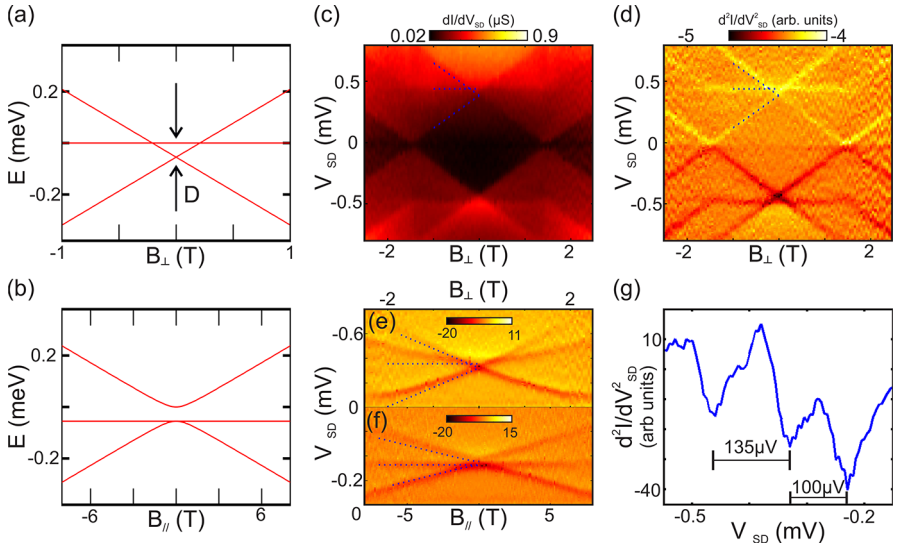

Figure 4. (color online) Evolution of HH triplet states from Hamiltonian (1) for (a) $B_\perp$ and (b) $B_\parallel$, using $g_\parallel = 0.57$, $g_\perp = 4.56$, and $D = 55$ μeV, as extracted from the measurements when the QD is in the singlet ground state, see Figure 3. (c) Experimental dI/dV_{SD} and (d) numerical derivative d^2I/dV_{SD}^2 as a function of $B_\perp$ and V_{SD}. The latter shows the ZFS more clearly; the calculation of (a) is plotted as dotted lines. (e, f) Numerical derivative d^2I/dV_{SD}^2 for a second device as a function of V_{SD} and $B_\perp$, $B_\parallel$, respectively. (g) Plot showing a line scan from (f) taken at $B_\parallel = -3.1$ T illustrating the unequal spacing of the triplet states. In this device a ZFS of 35 ± 5 μeV is observed; again, the dotted lines in (e) and (f) are calculated based on the experimentally extracted parameters ($g_\parallel = 0.52 \pm 0.13$, $g_\perp = 2.78 \pm 0.06$, and $D = 35$ μeV) without any additional fitting. The discrepancy in (e) is due to orbital effects[31] which are not taken into account in the model.

from Figure 3(b), and similar line traces at other $B_\parallel$'s. An even better agreement is obtained when freely adjusting D and $g_\parallel$ (not shown).

These considerations clearly show that there is a ZFS and that the magnetic field dependence shows a quite different behavior for $B_\parallel$ and $B_\perp$. If we have an odd number of electrons, the doublet could also be described with Hamiltonian (1). But in this case, both $S_\perp = \pm 1/2$ states have the same anisotropy energy. Hence, there is a Zeeman splitting but no ZFS as observed in Figure 3(a).

In order to further elucidate this behavior of the triplet state, we study in Figures 4 (c) and (d) the dependence on a magnetic field $B_\perp$. Using a second derivative to sharpen the features, it can be seen even more clearly that the HH triplet states are not degenerate at $B = 0$. Even more, the magnetic field evolution perfectly fits with that of Figure 4(a), which is also indicated as dashed (blue) lines. Figure 4 (e, f) shows the same split degeneracy also for a second device. In this case orbital effects also lead to a slight bending of the states for $B_\perp$,[a] and the ZFS is extracted to be 30 μeV. Except for this extra bending Figure 4 (e) resembles Figure 4(a) and Figure 4 (f) resembles Figure 4(b) for the two different magnetic field directions. From the observed splitting it is obvious that the ZFS needs to be taken into account when considering the energy band diagram of double QDs, for which it has been assumed so far that triplet HH states are all degenerate at $B = 0$ T.

In conclusion, we have demonstrated the ZFS for heavy-hole states confined in a two-dimensional quantum dot. Specifically, the triplet states are split into a double and a single degenerate level. This is not only of fundamental interest but also needs to be taken into account, for better or for worse, when operating heavy-hole qubits. As the studied hut wires are elongated we expect that our observation should be valid also for a double quantum dot potential. That is, also triplet (1,1) states, important for singlet–triplet qubits, should show a ZFS. In addition, it can be exploited for rotating and preparing a well-defined quantum state using Rabi oscillations at the ZFS (microwave) frequency, similar as for nitrogen vacancy centers in diamond.[36,37] A small magnetic field can further help addressing the spin ±1 states individually. If we consider the anisotropic exchange J_A as the origin of the ZFS, it can be employed for qubit operations[35] but may also be tuned (more) isotropic using proper pulse shaping.[34,38]

AUTHOR INFORMATION

Corresponding Author

Georgios Katsaros – *Institute of Science and Technology Austria, 3400 Klosterneuburg, Austria;* orcid.org/0000-0001-8342-202X; Phone: +43 2243 9000 2023; Email: georgios.katsaros@ist.ac.at

Authors

Josip Kukučka – *Institute of Science and Technology Austria, 3400 Klosterneuburg, Austria*

Lada Vukušić – *Institute of Science and Technology Austria, 3400 Klosterneuburg, Austria;* orcid.org/0000-0003-2424-8636

Hannes Watzinger – *Institute of Science and Technology Austria, 3400 Klosterneuburg, Austria*

Fei Gao – *Beijing National Laboratory for Condensed Matter Physics, Institute of Physics, Chinese Academy of Sciences, 100190 Beijing, China*

Ting Wang – *Beijing National Laboratory for Condensed Matter Physics, Institute of Physics, Chinese Academy of Sciences, 100190 Beijing, China;* orcid.org/0000-0002-4619-9575

Jian-Jun Zhang – *Beijing National Laboratory for Condensed Matter Physics, Institute of Physics, Chinese Academy of Sciences, 100190 Beijing, China; CAS Center for Excellence in Topological Quantum Computation, University of Chinese Academy of Sciences, 100049 Beijing, China*

https://dx.doi.org/10.1021/acs.nanolett.0c01466
Nano Lett. 2020, 20, 5201−5206

Karsten Held − *Institute of Solid State Physics, Vienna University of Technology, 1040 Vienna, Austria*

Complete contact information is available at: https://pubs.acs.org/10.1021/acs.nanolett.0c01466

Notes

The authors declare no competing financial interest.

■ ACKNOWLEDGMENTS

We acknowledge G. Burkard, V. N. Golovach, C. Kloeffel, D. Loss, P. Rabl, and M. Rančić for helpful discussions. We further acknowledge T. Adletzberger, J. Aguilera, T. Asenov, S. Bagiante, T. Menner, L. Shafeek, P. Taus, P. Traunmüller, and D. Waldhäusl for their invaluable assistance. This research was supported by the Scientific Service Units of IST Austria through resources provided by the MIBA Machine Shop and the nanofabrication facility, by the FWF-P 32235 project, by the National Key R&D Program of China (2016YFA0301701, 2016YFA0300600), and by the European Union's Horizon 2020 research and innovation program under grant agreement no. 862046. All data of this publication are available at 10.15479/AT:ISTA:7689.

■ ADDITIONAL NOTE

[a]That is, the magnetic flux alters the wave function (and hence energies) of the states in the quantum dot on top of the Zeeman splitting. This can be described, e.g., when calculating the Fock−Darwin states. For illustrations as well as for comparisons of this bending with experiment, we refer the reader to the review in ref 31.

■ REFERENCES

(1) Hao, X.-J.; Tu, T.; Cao, G.; Zhou, C.; Li, H.-O.; Guo, G.-C.; Fung, W. Y.; Ji, Z.; Guo, G.-P.; Lu, W. Strong and Tunable SpinOrbit Coupling of One-Dimensional Holes in Ge/Si Core/Shell Nanowires. *Nano Lett.* **2010**, *10*, 2956−2960.

(2) *Spin-Orbit Coupling Effects in Two-Dimensional Electron and Hole Systems*; Winkler, R., Ed.; Springer: New York, 2003.

(3) Kloeffel, C.; Trif, M.; Loss, D. Strong spin-orbit interaction and helical hole states in Ge/Si nanowires. *Phys. Rev. B: Condens. Matter Mater. Phys.* **2011**, *84*, 195314.

(4) Liu, H.; Marcellina, E.; Hamilton, A. R.; Culcer, D. Strong spin-orbit interaction and helical hole states in Ge/Si nanowires. *Phys. Rev. Lett.* **2018**, *121*, 087701.

(5) Maurand, R.; Jehl, X.; Kotekar-Patil, D.; Corna, A.; Bohuslavskyi, H.; Laviéville, R.; Hutin, L.; Barraud, S.; Vinet, M.; Sanquer, M.; De Franceschi, S. A CMOS silicon spin qubit. *Nat. Commun.* **2016**, *7*, 13575.

(6) Watzinger, H.; Kukučka, J.; Vukušić, L.; Gao, F.; Wang, T.; Schäffler, F.; Zhang, J. J.; Katsaros, G. A germanium hole spin qubit. *Nat. Commun.* **2018**, *9*, 3902.

(7) Hendrickx, N. W.; Franke, D. P.; Sammak, A.; Scappucci, G.; Veldhorst, M. Fast two-qubit logic with holes in germanium. *Nature* **2020**, *577*, 487.

(8) Crippa, A.; Ezzouch, R.; Aprá, A.; Amisse, A.; Laviéville, R.; Hutin, L.; Bertrand, B.; Vinet, M.; Urdampilleta, M.; Meunier, T.; Sanquer, M.; Jehl, X.; Maurand, R.; De Franceschi, S. Gate-reflectometry dispersive readout and coherent control of a spin qubit in silicon. *Nat. Commun.* **2019**, *10*, 2776.

(9) Golovach, V. N.; Borhani, M.; Loss, D. Electric-dipole-induced spin resonance in quantum dots. *Phys. Rev. B: Condens. Matter Mater. Phys.* **2006**, *74*, 165319.

(10) Kato, Y.; Myers, R. C.; Driscoll, D. C.; Gossard, A. C.; Levy, J.; Awschalom, D. D. Gigahertz Electron Spin Manipulation Using Voltage-Controlled g-Tensor Modulation. *Science* **2003**, *299*, 1201.

(11) Crippa, A.; Maurand, R.; Bourdet, L.; Kotekar-Patil, D.; Amisse, A.; Jehl, X.; Sanquer, M.; Laviéville, R.; Bohuslavskyi, H.; Hutin, L.; Barraud, S.; Vinet, M.; Niquet, Y.-M.; De Franceschi, S. Electrical Spin Driving by *g*-Matrix Modulation in Spin-Orbit Qubits. *Phys. Rev. Lett.* **2018**, *120*, 137702.

(12) Vukušić, L.; Kukučka, J.; Watzinger, H.; Milem, J. M.; Schäffler, F.; Katsaros, G. Single-Shot Readout of Hole Spins in Ge. *Nano Lett.* **2018**, *18*, 7141.

(13) Hendrickx, N. W.; Lawrie, W. I. L.; Petit, L.; Sammak, A.; Scappucci, G.; Veldhorst, M. A single-hole spin qubit. 2019, arXiv:1912.10426.

(14) Kloeffel, C.; Rančić, M. J.; Loss, D. Direct Rashba spin-orbit interaction in Si and Ge nanowires with different growth directions. *Phys. Rev. B: Condens. Matter Mater. Phys.* **2018**, *97*, 235422.

(15) Luttinger, J. M.; Kohn, W. Motion of Electrons and Holes in Perturbed Periodic Fields. *Phys. Rev.* **1955**, *97*, 869.

(16) Luttinger, J. M. Quantum Theory of Cyclotron Resonance in Semiconductors: General Theory. *Phys. Rev.* **1956**, *102*, 1030.

(17) Rau, I. G.; et al. Reaching the magnetic anisotropy limit of a 3d metal atom. *Science* **2014**, *344*, 988.

(18) Jacobson, P.; Herden, T.; Muenks, M.; Laskin, G.; Brovko, O.; Stepanyuk, V.; Ternes, M.; Kern, K. Quantum engineering of spin and anisotropy in magnetic molecular junctions. *Nat. Commun.* **2015**, *6*, 8536.

(19) Miyamachi, T.; et al. Stabilizing the magnetic moment of single holmium atoms by symmetry. *Nature* **2013**, *503*, 242.

(20) Gambardella, P.; Rusponi, S.; Veronese, M.; Dhesi, S. S.; Grazioli, C.; Dallmeyer, A.; Cabria, I.; Zeller, R.; Dederichs, P. H.; Kern, K.; Carbone, C.; Brune, H. Giant Magnetic Anisotropy of Single Cobalt Atoms and Nanoparticles. *Science* **2003**, *300*, 1130.

(21) Hirjibehedin, C. F.; Lin, C. Y.; Otte, A. F.; Ternes, M.; Lutz, C. P.; Jones, B. A.; Heinrich, A. J. Large Magnetic Anisotropy of a Single Atomic Spin Embedded in a Surface Molecular Network. *Science* **2007**, *317*, 1199.

(22) Hanson, R.; Kouwenhoven, L. P.; Petta, J. R.; Tarucha, S.; Vandersypen, L. M. K. Spins in few-electron quantum dots. *Rev. Mod. Phys.* **2007**, *79*, 1217−1265.

(23) Gao, F.; et al. Site-Controlled Uniform Ge/Si Hut Wires with Electrically Tunable Spin−Orbit Coupling. *Adv. Mater.* **2020**, *32*, 1906523.

(24) Zhang, J. J.; Katsaros, G.; Montalenti, F.; Scopece, D.; Rezaev, R. O.; Mickel, C.; Rellinghaus, B.; Miglio, L.; De Franceschi, S.; Rastelli, A.; Schmidt, O. G. Monolithic Growth of Ultrathin Ge Nanowires on Si(001). *Phys. Rev. Lett.* **2012**, *109*, 085502.

(25) Katsaros, G.; Golovach, V. N.; Spathis, P.; Ares, N.; Stoffel, M.; Fournel, F.; Schmidt, O. G.; Glazman, L. I.; De Franceschi, S. Observation of spin-selective tunneling in SiGe nanocrystals. *Phys. Rev. Lett.* **2011**, *107*, 246601.

(26) Watzinger, H.; Kloeffel, C.; Vukušić, L.; Rossell, M. D.; Sessi, V.; Kukučka, J.; Kirchschlager, R.; Lausecker, E.; Truhlar, A.; Glaser, M.; Rastelli, A.; Fuhrer, A.; Loss, D.; Katsaros, G. Heavy-Hole States in Germanium Hut Wires. *Nano Lett.* **2016**, *16*, 6879.

(27) Kogan, A.; Amasha, S.; Goldhaber-Gordon, D.; Granger, G.; Kastner, M. A.; Shtrikman, H. Measurements of Kondo and Spin Splitting in Single-Electron Transistors. *Phys. Rev. Lett.* **2004**, *93*, 166602.

(28) De Franceschi, S.; Sasaki, S.; Elzerman, J. M.; van der Wiel, W. G.; Tarucha, S.; Kouwenhoven, L. P. Electron Cotunneling in a Semiconductor Quantum Dot. *Phys. Rev. Lett.* **2001**, *86*, 878−881.

(29) Katsaros, G.; Spathis, P.; Stoffel, M.; Fournel, F.; Mongillo, M.; Bouchiat, V.; Lefloch, F.; Rastelli, A.; Schmidt, O. G.; De Franceschi, S. Hybrid superconductor−semiconductor devices made from self-assembled SiGe nanocrystals on silicon. *Nat. Nanotechnol.* **2010**, *5*, 458−464.

(30) Nenashev, A.; Dvurechenskii, A.; Zinovieva, A. Wave functions and g factor of holes in Ge/Si quantum dots. *Phys. Rev. B: Condens. Matter Mater. Phys.* **2003**, *67*, 205301.

(31) Kouwenhoven, L. P.; Austing, D. G.; Tarucha, S. Few-electron quantum dots. *Rep. Prog. Phys.* **2001**, *64*, 701.

(32) Misiorny, M.; Hell, M.; Wegewijs, W. R. *Nat. Phys.* **2013**, *9*, 801.
(33) Bruno, P. Chapter 24: Physical Origins and Theoretical Models of Magnetic Anisotropy. *IFF-Ferienkurs Forschungszentrum Jülich*; 1993; ISBN 3893361103.
(34) Burkard, G.; Loss, D. Cancellation of Spin-Orbit Effects in Quantum Gates Based on the Exchange Coupling in Quantum Dots. *Phys. Rev. Lett.* **2002**, *88*, 047903.
(35) Shim, Y.-P.; Oh, S.; Hu, X.; Friesen, M. Controllable Anisotropic Exchange Coupling between Spin Qubits in Quantum Dots. *Phys. Rev. Lett.* **2011**, *106*, 180503.
(36) Fuchs, G. D.; Dobrovitski, V. V.; Toyli, D. M.; Heremans, F. J.; Awschalom, D. D. Gigahertz Dynamics of a Strongly Driven Single Quantum Spin. *Science* **2009**, *326*, 1520−1522.
(37) Jelezko, F.; Wrachtrup, J. Single defect centres in diamond: A review. *Phys. Status Solidi A* **2006**, *203*, 3207−3225.
(38) Bonesteel, N. E.; Stepanenko, D.; DiVincenzo, D. P. Anisotropic Spin Exchange in Pulsed Quantum Gates. *Phys. Rev. Lett.* **2001**, *87*, 207901.

https://dx.doi.org/10.1021/acs.nanolett.0c01466
Nano Lett. 2020, 20, 5201−5206